

1.2

A COMPARISON OF ISNET DATA WITH RADAR DATA FOR TORNADIC AND POTENTIALLY TORNADIC STORMS IN NORTHEAST COLORADO

Edward J. Szoke*

NOAA Research–Forecast Systems Laboratory, Boulder, Colorado

*in collaboration with the Cooperative Institute for Research in the Atmosphere (CIRA)

Alfred J. Bedard, Jr.

NOAA Environmental Technology Laboratory, Boulder, Colorado

Eric Thaler and Robert Glancy

NOAA National Weather Service Forecast Office, Boulder, Colorado

1. INTRODUCTION

One of the key responsibilities of the National Weather Service (NWS) is the issuance of timely warnings for tornadoes. Enormous advances were made in the ability to issue tornado warnings with the implementation of Doppler radars across the nation. The use of Doppler radar data, coupled with comprehensive Weather Forecast Office (WFO) coordinated volunteer storm spotter information, has enabled forecasters to issue many life-saving tornado warnings.

Nevertheless, there are still many issues that conspire to add difficulty to issuing reliable tornado warnings, ranging from being able to resolve important radar velocity signals to nonsupercell tornadogenesis (Brady and Szoke 1989; Wakimoto and Wilson, 1989). In addition, it is well known that the actual formation of a tornado from supercell storms, with their mesocyclone signatures that are detected so well by Doppler radar, is still not fully understood, and with key aspects that may be impossible to detect from the current array of Doppler radars. The effort to reduce the number of false alarms that is a consequence of this dilemma is another extremely important issue (Brooks 2004). With these and other aspects a part of the challenges to issuing tornado warnings, any type of additional information is useful. A potential system that may provide such additional information is a passive system that senses infrasonic sound, known as ISNet.

The ISNet system is discussed in detail in other papers at this conference, as is the network that was in place during the convective seasons of 2003 and 2004 (Bedard et al. 2004). The purpose of this research is to gain an understanding of how the signals received by the system compare to radar information that a NWS forecaster uses in

issuing tornado warnings, and from this to determine what, if any, added value can be obtained from the ISNet data. Numerous cases have been collected that clearly indicate that infrasonic signals arise from tornadic and other storms. However, detailed analysis has not been done to correlate these signals with detailed Doppler radar data as well as visual observations. It is hoped that this preliminary study can begin to fill this gap and help to better evaluate whether ISNet data can be a useful addition to the information a forecaster needs to issue tornado warnings.

2. ANALYSIS METHODOLOGY

The procedure used for this paper is outlined below. Two cases are discussed here, with one having a detailed radar analysis. We plan on completing a detailed radar analysis for the second case, as well as adding one or more cases for the presentation at the conference. Because this is a system in its infancy in terms of evaluating its potential use, both the types of data displays and what the data might be showing will be illustrated.

A case with tornadoes and other severe weather in the area of responsibility for the Boulder, Colorado WFO from 9 June 2004 was selected for analysis. There were actually several apparent nonsupercell tornadoes relatively close to the radar, followed by more organized storms, one of which produced a strong tornado farther from the radar in the northeast corner of Colorado. This case is somewhat complex in the number of storms occurring, and for the initial detailed comparison of ISNet data with radar data, we chose a more straightforward system from 20-21 May 2004. The details of both cases are discussed in the next section, with the ISNet display currently used most generally by the forecasters, as well as some other displays that are not yet available routinely. The individual storm on 20-21 May is examined and a time-height series of differential Doppler velocity constructed. This forms the baseline for comparison with a time series presentation of the ISNet data and is the

*Corresponding author address: Ed Szoke, NOAA/OAR/FSL, R/FS1, 325 Broadway, Boulder, CO 80305; e-mail: Edward.J.Szoke@noaa.gov

main basis for attempting to determine how the infrasound signals relate to standard measurements of storm or smaller scale rotation. Storm spotter reports are also used, and for our presentation at the conference, photos will be added for some of the events.

3. 20-21 MAY 2004 CASE

This day was chosen for the initial detailed comparison of ISNet data with radar data because it was a relatively straightforward evolution of a single supercell that began close to the radar near 0000 UTC on 21 May, and then moved east-northeast over the next four hours. The severe reports for this case are shown in Fig. 1. One complicating factor for this case is that although three tornadoes were reported, upon further review

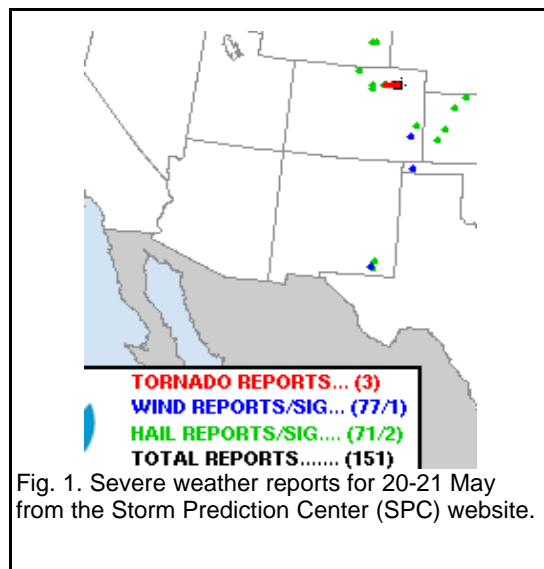


Fig. 1. Severe weather reports for 20-21 May from the Storm Prediction Center (SPC) website.

of other storm chaser reports, a final determination was made that there apparently were no tornado touchdowns. Judging by the radar data to be shown, the storm was certainly capable of producing tornadoes during the time of the reports, and whether they in fact occurred remains uncertain.

The atmosphere on 20 May was not only very unstable, but also possessed strong vertical wind shear, as shown in the evening sounding from Denver, Colorado (Fig. 2), and by profiler data from the Platteville, Colorado site, located ~40 km to the north (Fig. 3). Both locations were very close to where the storm of interest originated just before 0000 UTC, which was just to the northwest of Denver's International Airport and roughly between the Platteville profiler site and the sounding site (at the old Denver airport). These conditions are not unusual for May in Colorado, and clearly were sufficient to support supercell storms. An overview of surface conditions with a visible satellite image is shown in Fig. 4. Southeast low-level flow had created a Denver Cyclone (Szoke et al. 1984) and a subsequent

convergence zone that acted as a focal point for storm initiation. The line of towering cumuli between the Platteville profiler and Denver sounding sites in Fig. 4 also developed in an area of more abundant sunshine. The development along the convergence zone actually consisted of several cells, with a couple briefly reaching 50 dBZ maximum echo strength. Although these initial cells did not survive the strongly sheared environment, the last cloud to develop along the line shortly after 2330 UTC did, and quickly became a very strong and visually impressive storm. The radar images in Fig. 5 shows a history of the storm over the next few hours as it moved off to the east-northeast. This track took it just to the north of Interstate 76, making it easy to observe for several storm chasers, before eventually crossing the interstate just after dark well to the northeast of Denver. Although in an ideal position for visual observation, the possible tornado development is still somewhat uncertain because it was nearing dark (and continuing into nighttime) when the tornado sightings were reported.

As seen in the radar imagery in Fig. 5, the storm developed very rapidly, and within an hour of initiation had produced severe hail (0.75 in or greater), with the first report at 0031 UTC. Subsequent severe hail reports continued through 0330 UTC. Some of the maximum sized hail reported occurred at 0211 UTC (1.75 in diameter hail), 0310 UTC, another 1.75 in report, and at 0330 UTC (2.0 in). The tornado reports that came in that evening to the Boulder Weather Forecast Office (WFO) began with a brief tornado reported at 0218 UTC, followed by another tornado at 0229 UTC, then the final report (a brief touchdown) at 0330 UTC. Again, using collaborating observations, a final determination was made that there was no "official" tornado from this storm, but because it is often difficult to find any damage tracks in the relatively sparsely populated region east of the Front Range, and the fact that darkness was setting in during the 0200 to 0230 UTC period, it is difficult to say with complete reliability that a tornado was never produced by this supercell. In fact, as will be shown in a detailed radar analysis of the storm, there was a strong mesocyclone for most of the storm's lifetime, and a number of volume scans where a tornado vortex signature (TVS) was identified by the National Weather Service (NWS) storm algorithm.

The ISNet display that was available to forecasters at the Boulder WFO, via an internet connection to NOAA's Environmental Technology Laboratory (ETL) in Boulder, is shown in the imagery in Fig. 6. Details of this imagery and what it means in terms of infrasonic signal are discussed by Bedard et al. (2004, this volume). Training was given to forecasters at the Boulder WFO prior to the onset of severe weather season. The basic display consists of a circle

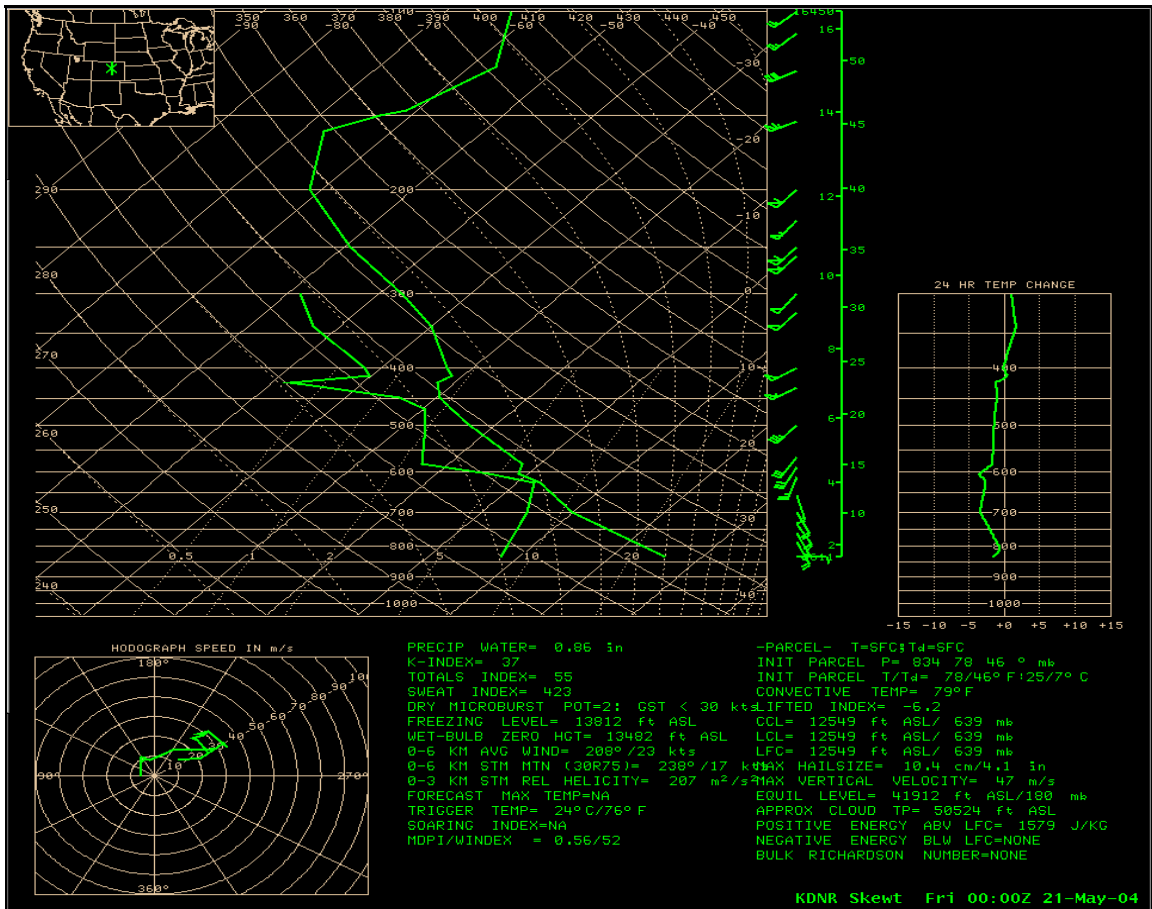


Fig. 2. Denver sounding for 0000 UTC on 21 May. A hodograph (in ms^{-1}) is also shown, as well as a number of parameters.

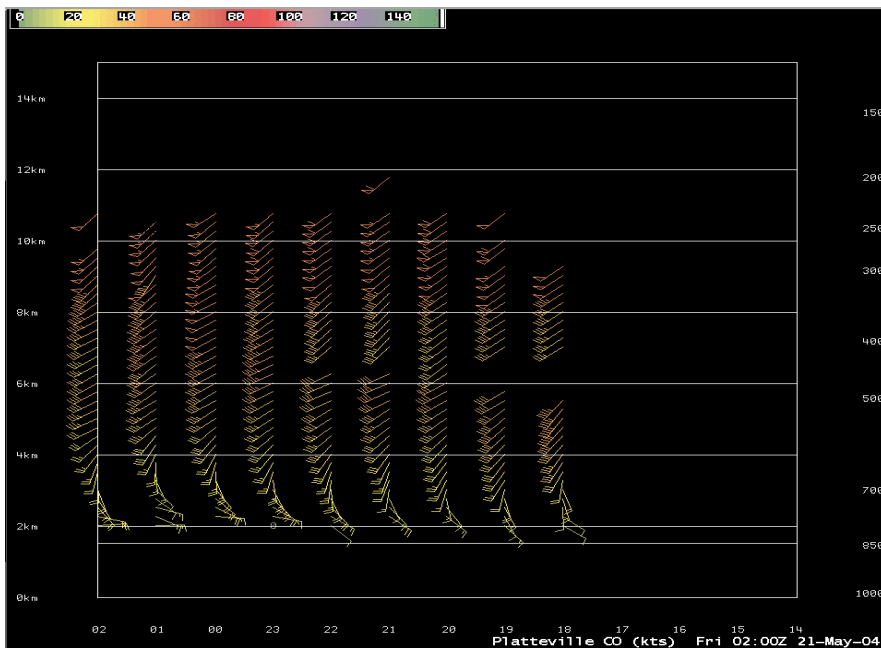


Fig. 3. Winds (knots) from the Platteville profiler, from 2100 UTC on 20 May to 0300 UTC on 21 May, versus height (km MSL, left side, with equivalent pressure scale, in mb, on the right).

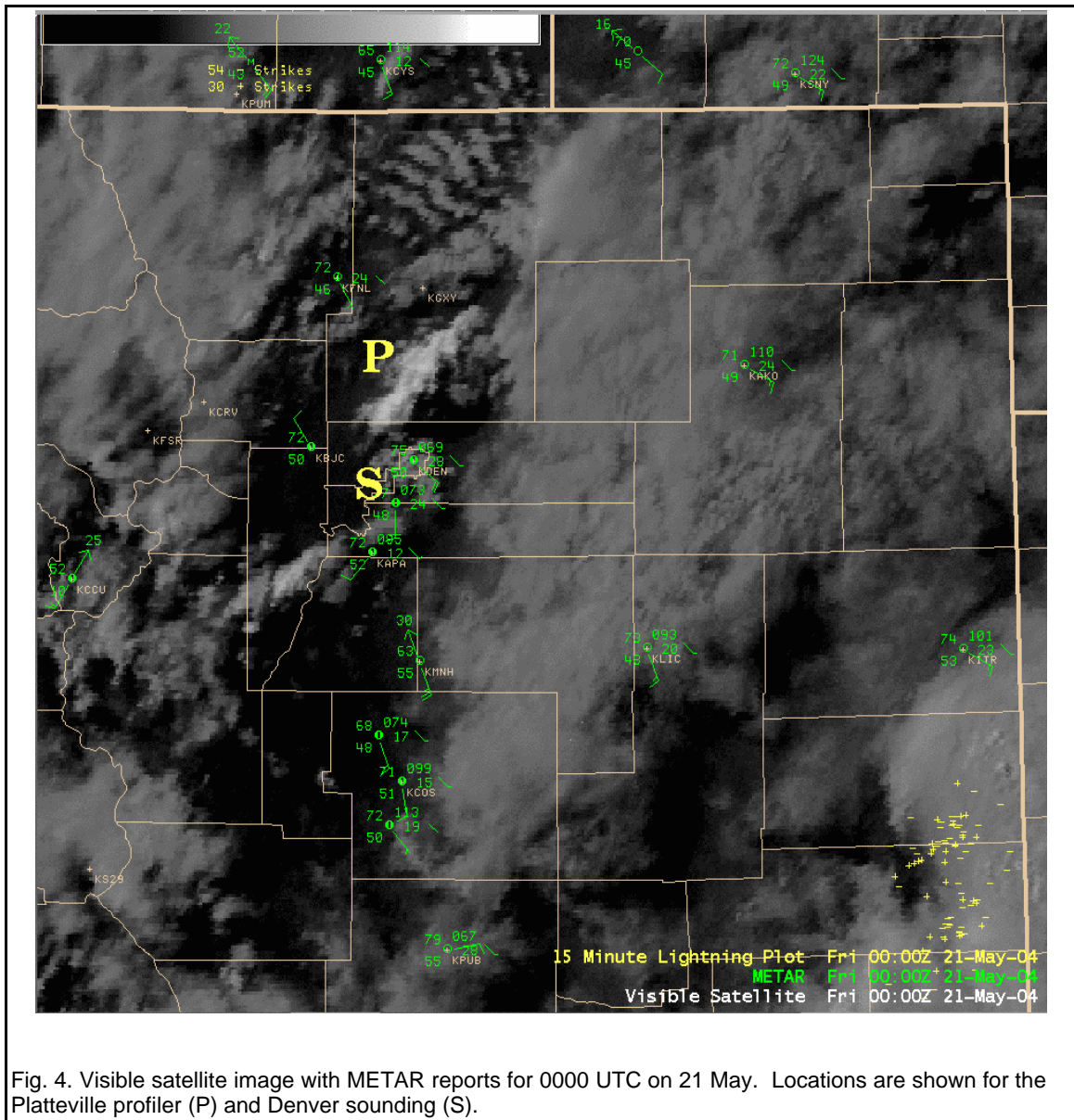


Fig. 4. Visible satellite image with METAR reports for 0000 UTC on 21 May. Locations are shown for the Platteville profiler (P) and Denver sounding (S).

around the local infrasound site, located at Erie, Colorado, which is about 15 km south of the Platteville profiler site. Also shown are the other two infrasound sites that make up the current network, one collocated with the Pueblo WFO, and the other with the Goodland, Kansas WFO (for this event the Goodland site was not operational). The dots emanating from each site and located on and away from the circle represent the quality of the signal, with the highest quality signal in red, representing a correlation coefficient greater than 0.6, a “good” quality signal in yellow (correlation coefficient from 0.5 to 0.6), and the other dots for correlation coefficients between 0.4 and 0.5. The time period for the display is approximately one hour, updated every 5 min, with newer signals in brighter shades of the appropriate color. Should there be a signal received from a particular storm, there would be an accumulation of points away

from the circle, in the direction towards the storm. Since infrasonic signals can travel great distances, it is often necessary to triangulate using the other sites to be more certain of where the signal is coming from.

The display shown in Fig. 6 was a first cut at a possible “operational” display for testing at the three WFOs, and while at times adequate, there were many other times when forecasters found it difficult to discern useful information from this particular display. Other displays are possible, including a display similar to Fig. 6 but for a histogram of the signal, with spurious signals removed. Additional displays that are possible include a time series that combines the azimuth of where a signal is emanating from along with the strength of the signal by color coding, using the same colors as in the plan view display in Fig. 6.

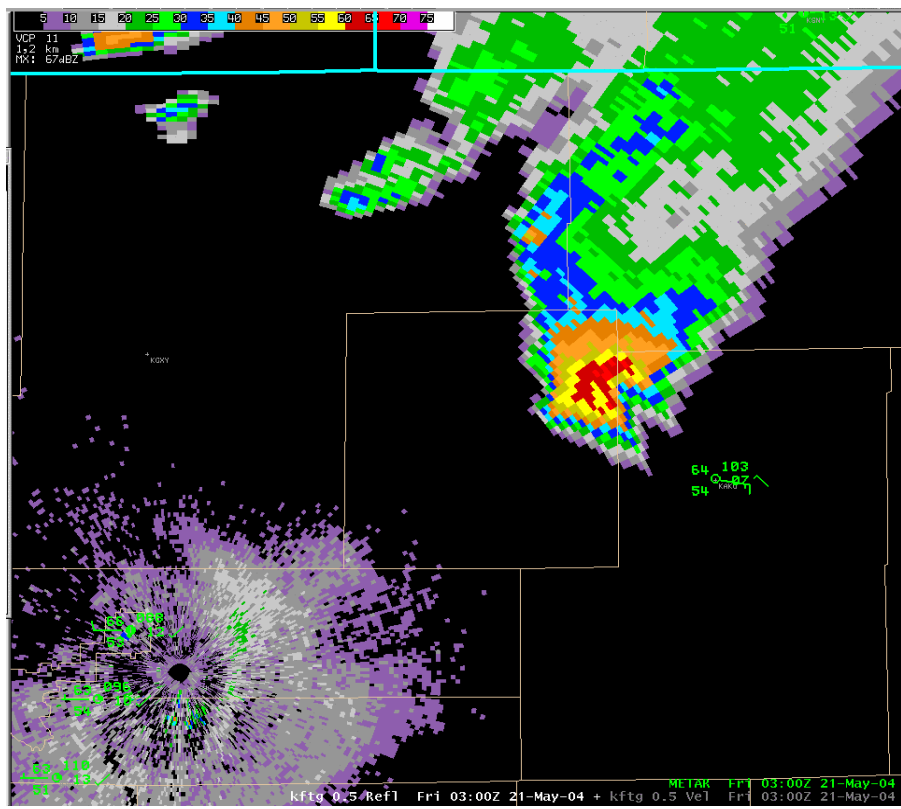
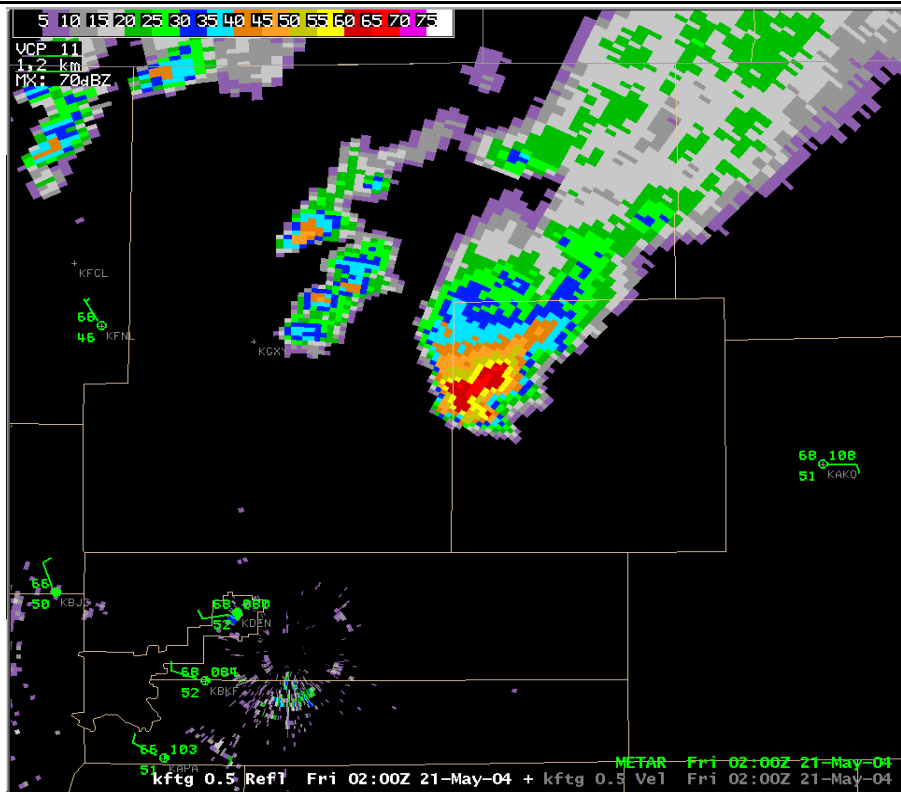
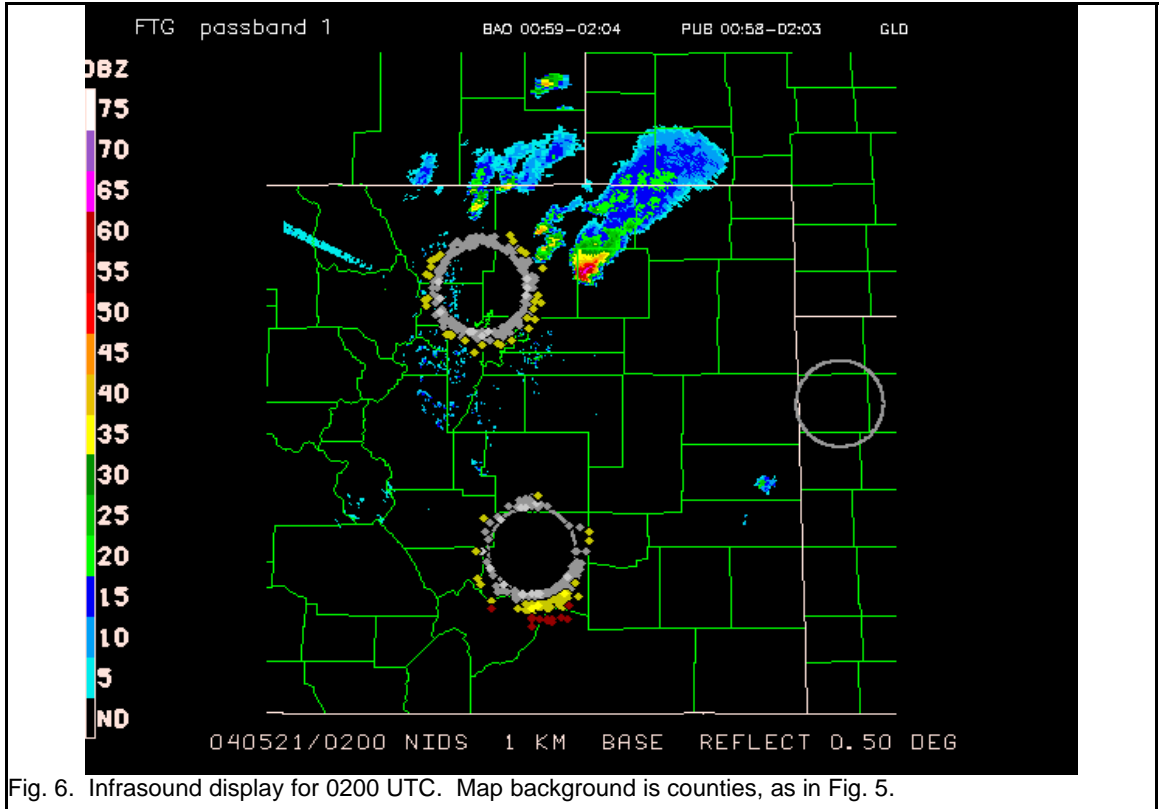
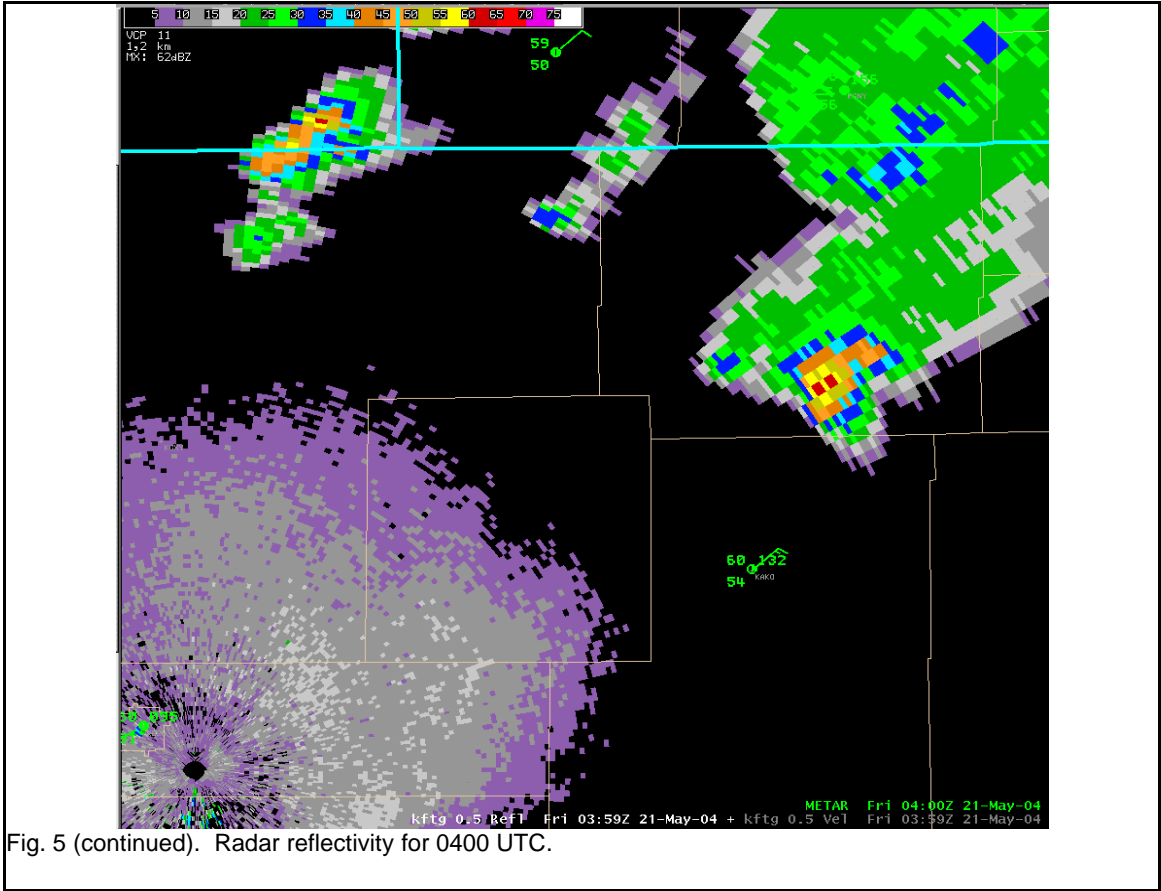


Fig. 5 (continued). Radar reflectivity for 0200 UTC (top) and 0300 UTC (bottom).



This type of display was also available operationally, for the local site, and is shown in Fig. 7. In this display, if there were a signal being received over time from a given location, the points would be gathered together along the azimuth toward the signal, with the quality of the signal indicated by the color of the stars in the display. For the 0200 UTC time, there had been no

UTC was reprocessed to include more of the lower signal points, and is displayed in Fig. 10. Even considering these lower correlation coefficient points, there is no really consistent signal for this time period seen in Fig. 10.

We will next present a detailed analysis of the evolution of the supercell in the form of two time-

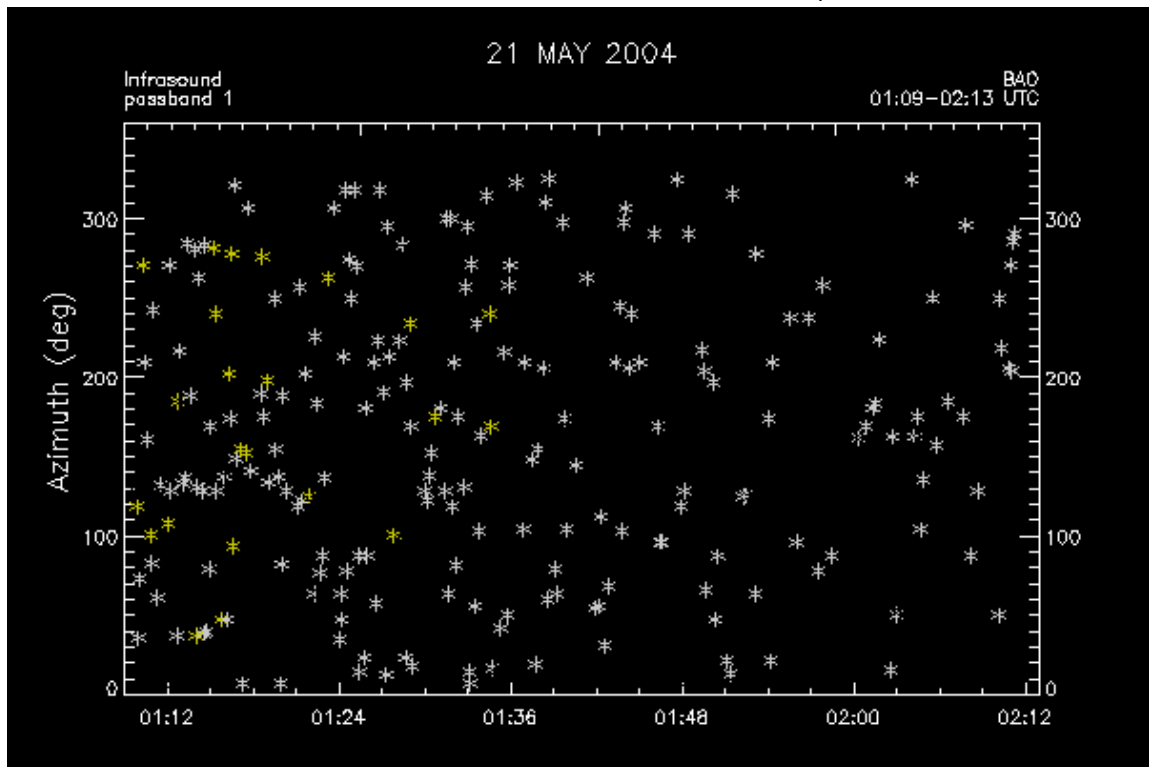


Fig. 7. Time series of infrasound signal for 1 h period ending at 0212 UTC.

consistent signal indicated on either display.

A similar set of figures is presented for the next hour ending near 0300 UTC, and including the time when the three tornadoes may have occurred. In Fig. 8 is the standard plan view display, and in Fig. 9 a time series display like that in Fig. 7. Again, neither display appears to indicate any reliable signal from this storm. The plan view display (Fig. 8) seems to indicate a possible signal from the Erie ISNet site for a storm somewhere to the north of the main supercell, although in fact this may be a signal from the strong storm since it is accumulated over a 1 h period. Pueblo is picking up a signal of some type but more from a northerly direction, perhaps from the cell near Cheyenne, Wyoming.

The time series display in Fig. 9 appears to contain some indication of a signal becoming more consistent over time from a direction of approximately 70 to 90 degrees, which would correspond to the direction of the supercell storm. The data for the one hour period ending at 0300

height cross-sections, following the type of analyses frequently used to illustrate the evolution of mesocyclones and other radar signatures. The first time series, shown in Fig. 11, gives the reflectivity history of the storm. Each radar angle was used to determine the maximum reflectivity of the storm over time. Fig. 12 is the same type of presentation but for the maximum differential velocity across the evolving mesocyclone, basically then the maximum toward added to maximum away, as determined by examining each radar angle for all the volume scans over the time period shown. There is some interpretation of course involved in this analysis, and care was taken to exclude some velocity measurements that occurred with extremely weak echo. The objective of these detailed analyses is to gain a better understanding of what the ISNet data is showing relative to rotation determined by Doppler radar, the standard warning tool currently used by the NWS. We will use additional types of ISNet displays not currently available to NWS forecasters at any of the test sites to better compare ISNet to the Doppler radar signals.

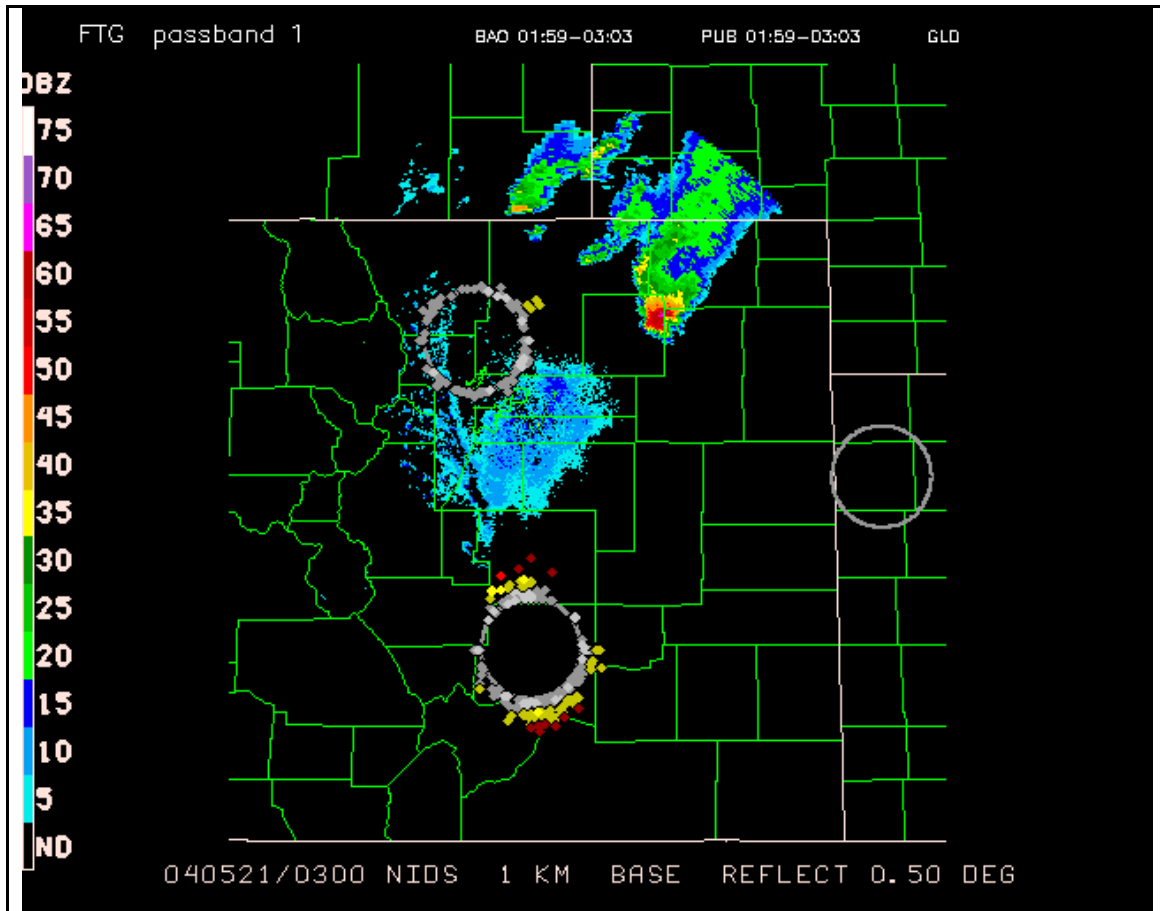


Fig. 8. Infrasound display, as in Fig. 6, for 0300 UTC.

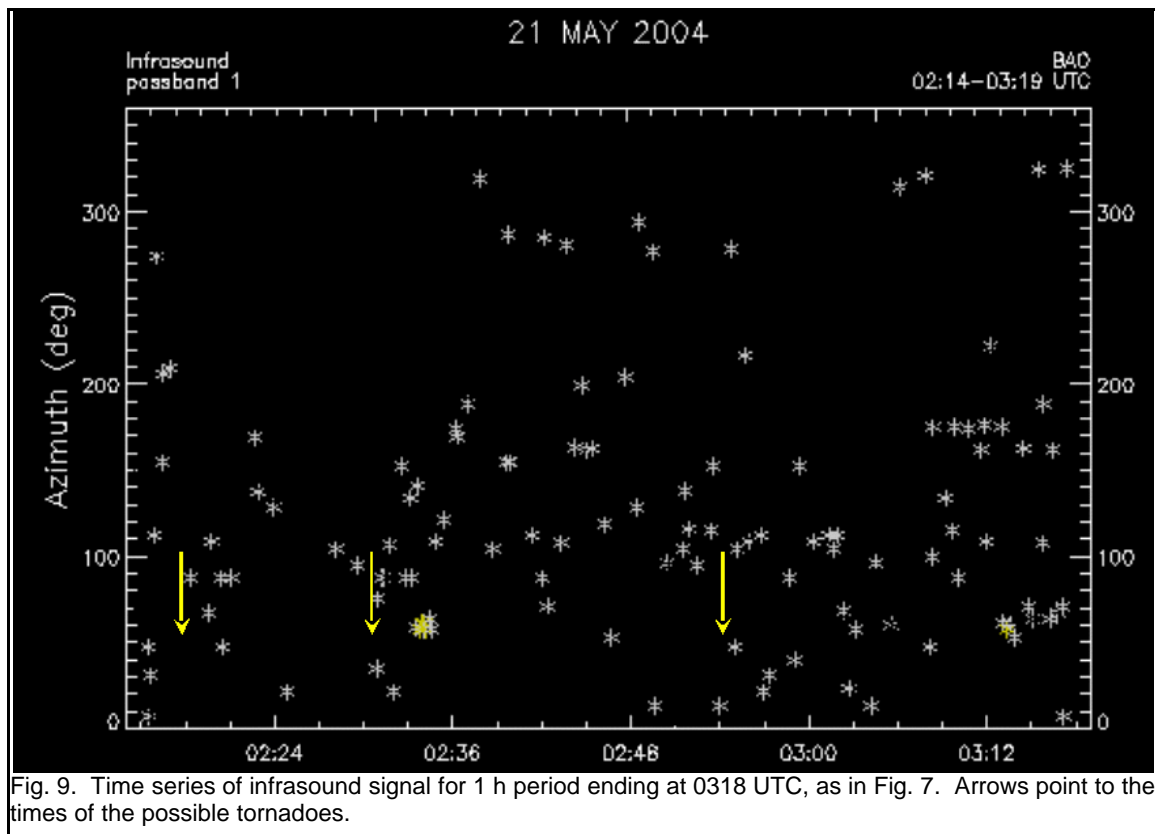
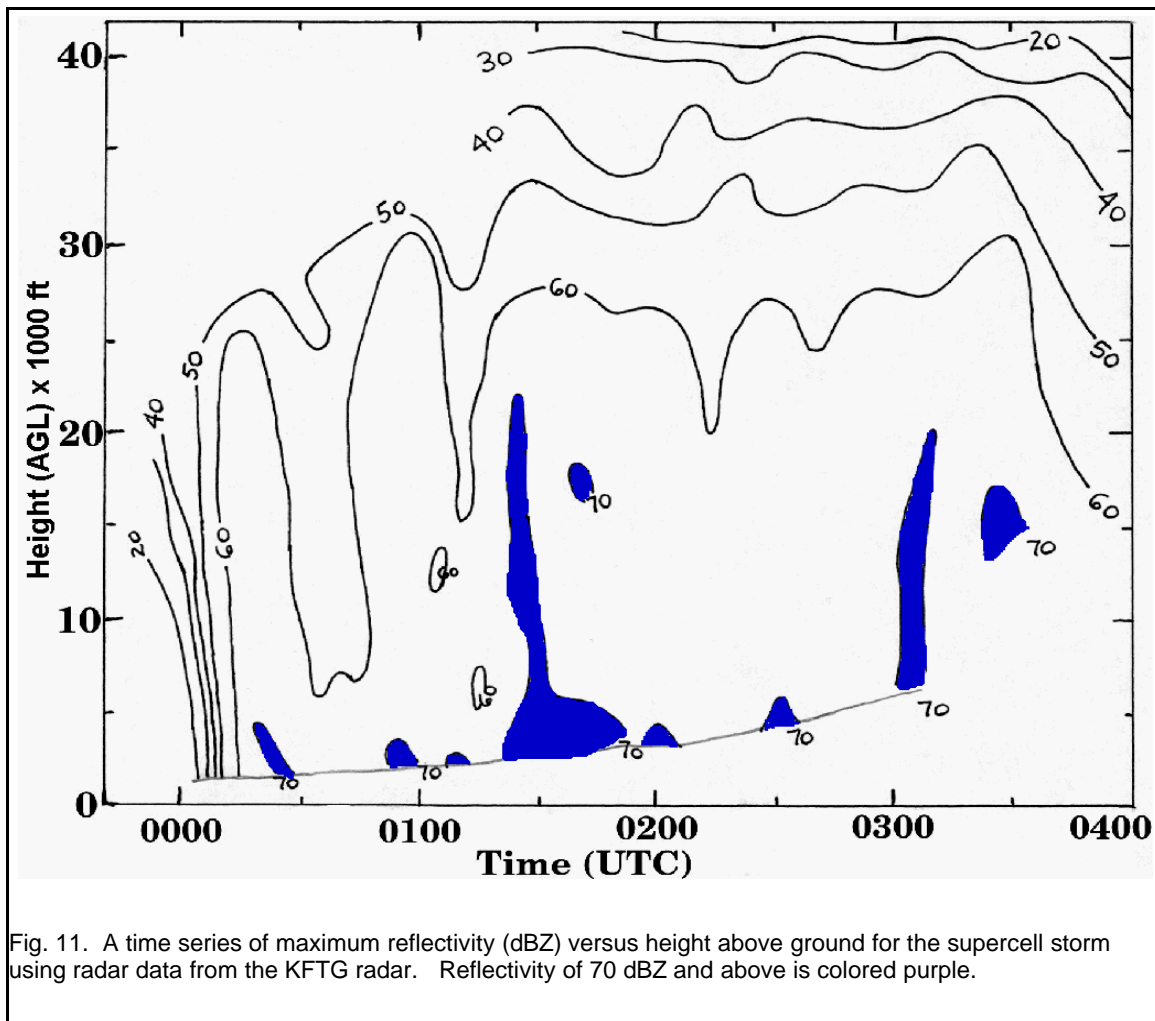
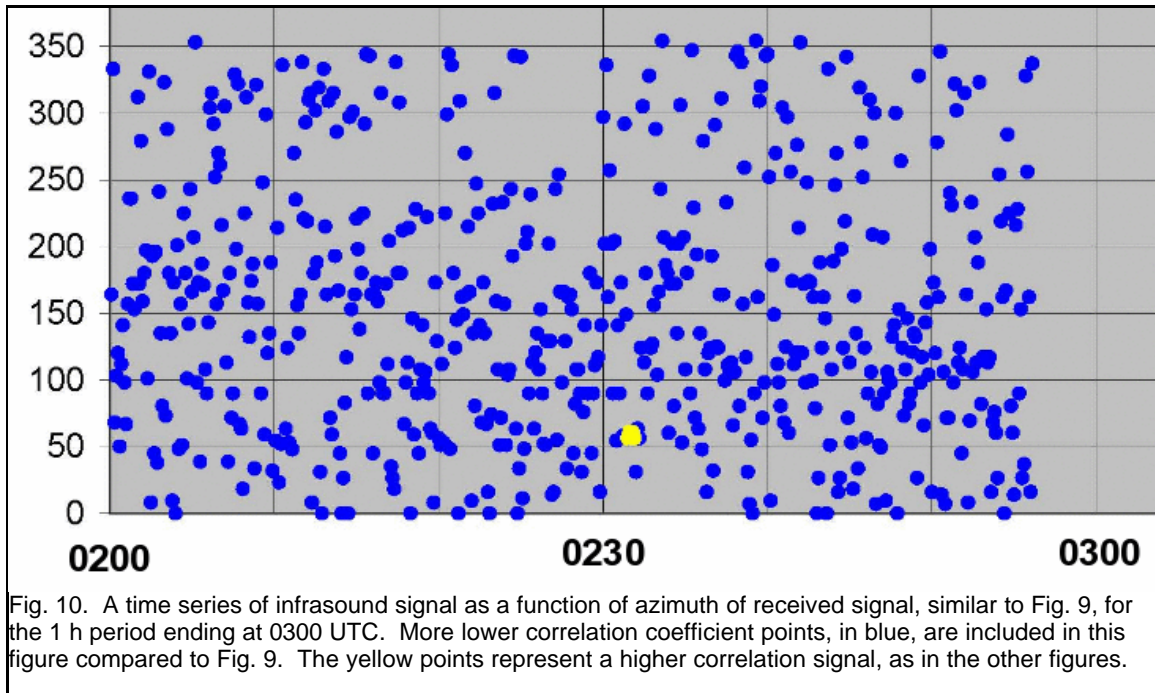


Fig. 9. Time series of infrasound signal for 1 h period ending at 0318 UTC, as in Fig. 7. Arrows point to the times of the possible tornadoes.



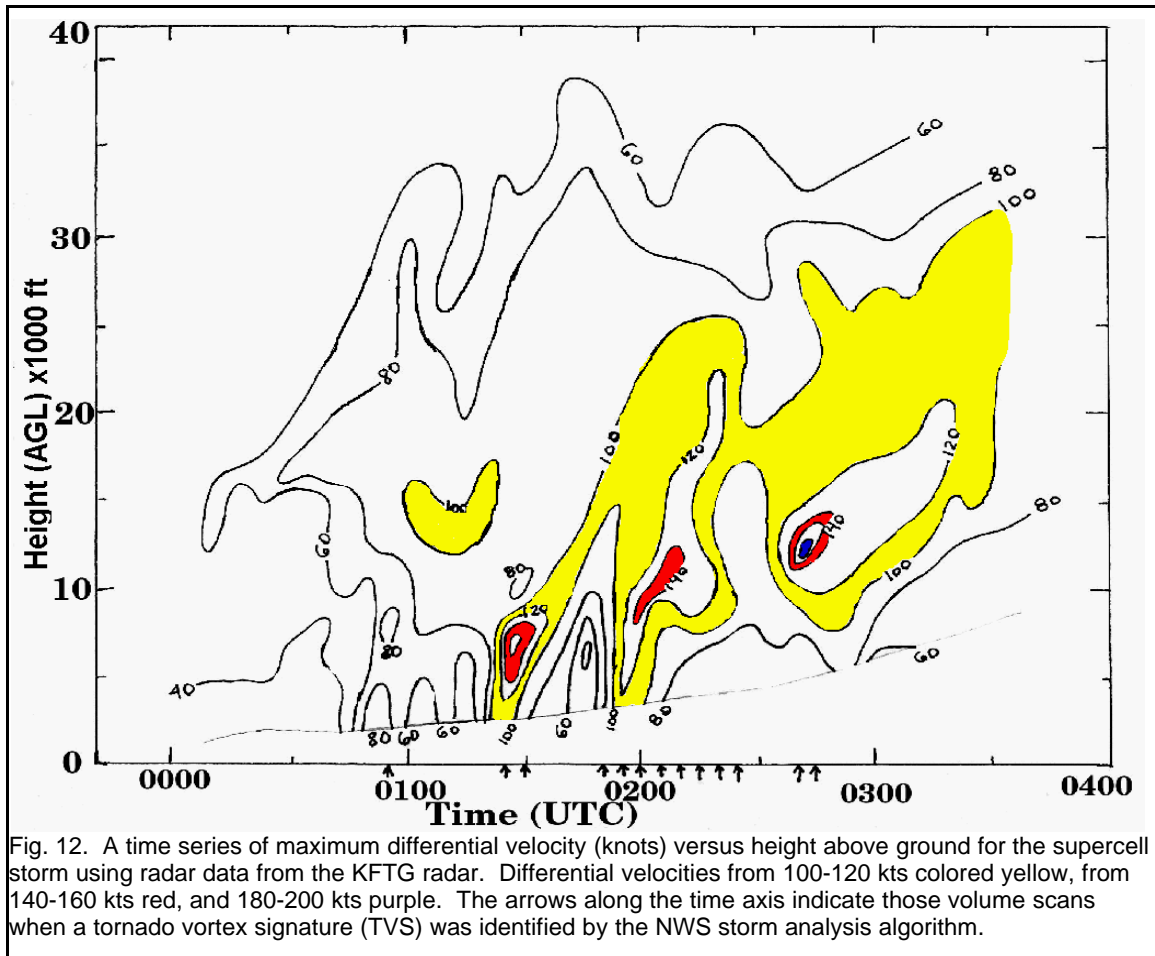


Fig. 12. A time series of maximum differential velocity (knots) versus height above ground for the supercell storm using radar data from the KFTG radar. Differential velocities from 100-120 kts colored yellow, from 140-160 kts red, and 180-200 kts purple. The arrows along the time axis indicate those volume scans when a tornado vortex signature (TVS) was identified by the NWS storm analysis algorithm.

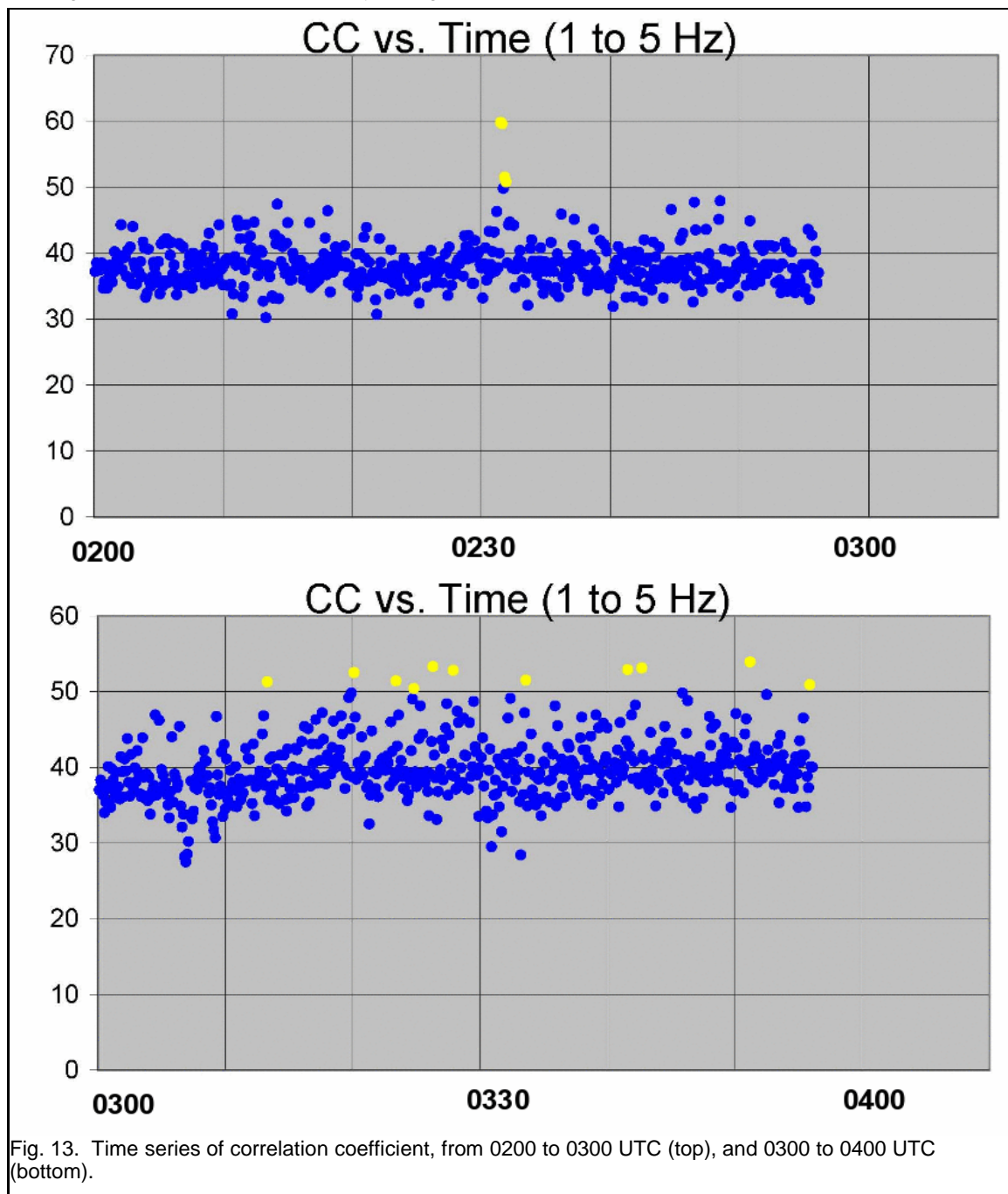
The most apparent feature in the reflectivity time series in Fig. 11 is the extremely rapid growth of the storm after its formation around 2345 UTC. This was also depicted in the plan view low-level radar scans in Fig. 5, and was quite obvious visually looking east at the storm from eastern Boulder. Weak rotation began quickly, with a more organized mesocyclone of 60 knots differential velocity appearing aloft near 15000 ft (AGL) by 0010 UTC. There is significant intensification of the mesocyclone after 0030 UTC, with a deep core of differential velocity greater than 80 knots at 0055 UTC, when the first TVS was indicated. At this time the storm spotters that reported the eventual tornadoes were seeing very strong inflow. Right after this, however, the low-level velocity couplet weakens, followed by a slight overall collapse of the storm itself (Fig. 11). This is just a temporary weakening, however, with significant strengthening of the storm just before 0130 UTC with a core of 70+ dBZ echo rising vertically to over 20000 ft AGL. Corresponding to this strengthening is a very strong increase in the low-level mesocyclone, with over 150 knots of differential velocity observed at 0125 UTC, and two consecutive periods of TVS signals. After another lull, the most consistently intense period of the storm begins, lasting for at least an hour, with a

very deep mesocyclone signal of over 100 knots of differential velocity extending from the lowest scan (now over 3000 feet above the surface as the storm moves away from the radar and into lower elevation) to near 25000 feet AGL. During this period there is a stretch of continuous TVS signals from the radar algorithm, and the three possible tornadoes. Tornado warnings were being issued at this time by the Boulder WFO. The storm continued to be quite strong after 0300 UTC, but moved into an area where it was difficult to discern a velocity signal at times because of range folding. It does appear that the lower level circulation did decrease, but the storm maintained a well-defined mid-level mesocyclone, continued to possess reflectivities up to 70 dBZ, and produce golf ball sized hail and strong winds up to 85 mph.

The ISNet information presented thus far did not show any significant consistent signals with this storm. In order to examine all possible infrasound signals that may have been received, several other displays were made. The display shown in the top part of Fig. 13 essentially is a time series presentation of the standard display, shown in Fig. 8. This display plots the correlation coefficient with time, and in this type of presentation the signal around 0230 stands out more clearly, certainly

when compared to both the plan view display like Fig. 8, but also the azimuth vs. time display shown in Fig. 9. There are more low signal points included in Fig. 13 compared to the display in Fig. 9, and this helps show the rise to the stronger signal near 0230 UTC. This display was not used for testing with the forecasters this year because it requires an additional display to determine what azimuth the signals are coming from. However, it is possible that this type of display, together with the standard plan view (Fig. 8), may be sufficient without an additional time series azimuth display. The signal around 0230 is still not very strong, and

actually comes after the most intense period of a low-level mesocyclone (Fig. 12) and follows the period of TVS signals. It is just after the time when the second possible tornado was observed, although correcting for the speed of sound and the distance to the storm at this time (~50 km) would shave about 2.5 min off that time and put it close to when this possible tornado occurred. Of the three tornadoes reported by the team of spotters, this was the only one that was not described as a "brief touchdown".



In the hour after 0300 UTC (bottom portion of Fig. 13) there are several signals that occur, not quite as strong as the one near 0230 UTC. A display of the azimuth of the received signal vs. time, shown in Fig. 14, indicates that a fairly consistent signal is being received from the supercell storm. Radar data continued to indicate a very strong storm with a well-defined mesocyclone, but without as much low-level circulation (though after 0300 UTC the lowest tilt was over 6000 ft AGL). Based on the radar data that we have, there is nothing definitive correlating this more consistent signal with any particular storm characteristic.

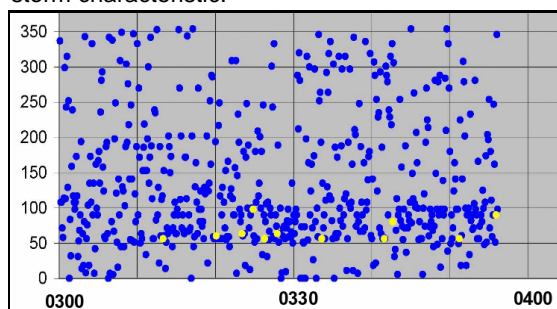


Fig. 14. Infrasound signal as a function of azimuth, as in Fig. 10, ending at 0400 UTC.

A final examination of this case is made by considering another potential type of display that may be tested during the next storm season. It is a plan view display like that currently in use, but is actually a histogram. Like the displays in Fig. 13,

the intent of this display is to better isolate any ISNet signals. The histogram display (described in Bedard et al. 2004) scales the data by the maximum number of points in a 5 degree azimuth bin size, to make the display more sensitive to lower-level but persistent signals that can appear more as noise in the current display (Figs. 6 and 8). Indeed, for this case a persistent signal does tend to be shown for the supercell storm. However, there are also other signals that are likely noise, but are about as prominently displayed. It is possible that additional processing may help eliminate some of this noise and result in a less confusing display.

In summary, the storm on the evening of 20 May was a classic supercell, ideally situated relatively close to the radar. It displayed a long-lived mesocyclone and triggered the TVS algorithm for a total period of about one hour of its lifetime. Fluctuations in the intensity of the mesocyclone were clearly observed by radar. Overall the ISNet signals for this case were not very strong. For the period of the best radar data, through 0320 UTC, there is only one real signal, occurring near 0230 UTC, about the time of a possible tornado. Actual tornado formation for this case is uncertain, with conflicting reports, although the radar time series of differential velocity certainly would support tornado formation. In his overview of cases examined largely from a more cursory look at radar and ISNet signals, Bedard et al. (2004) found no real signal with two significant large hail-producing supercell storms that did not produce tornadoes.

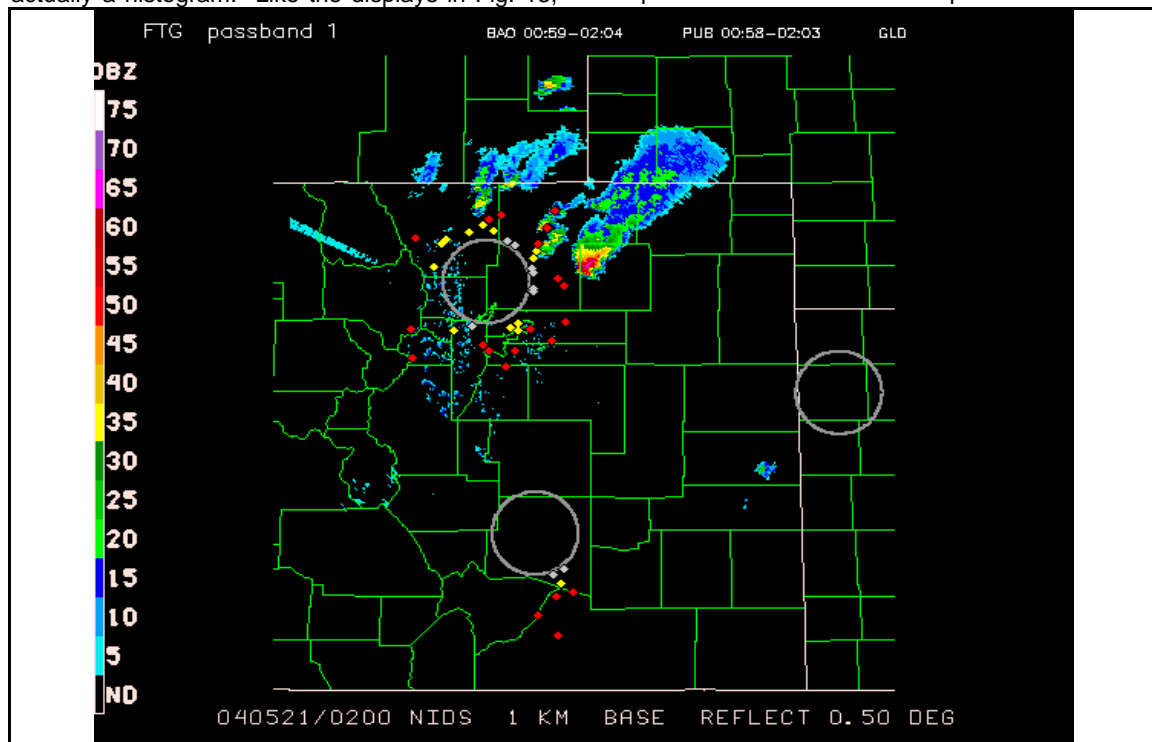


Fig. 14a. Histogram display for the ~1 h period ending at 0200 UTC. The color coding of the dots is identical in terms of correlation coefficient as in previous figures.

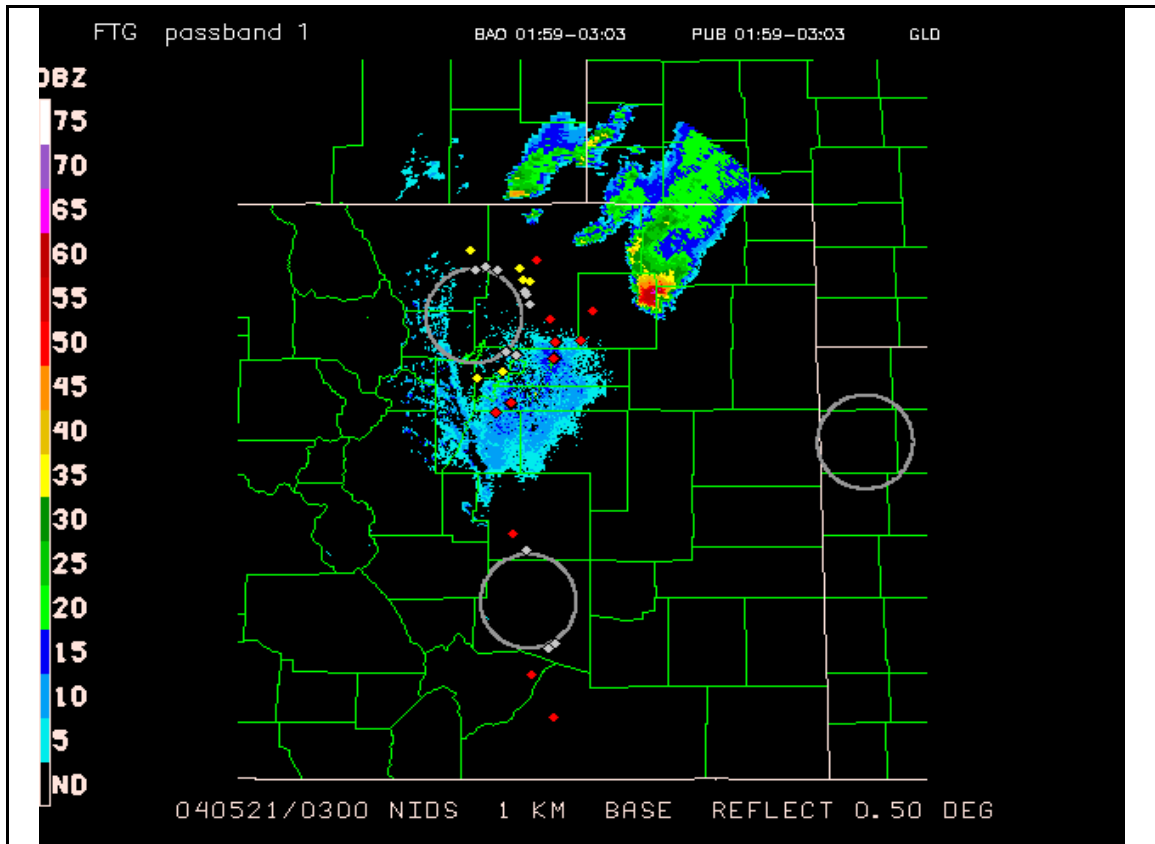


Fig. 14b. Histogram display for the ~1 h period ending at 0300 UTC.

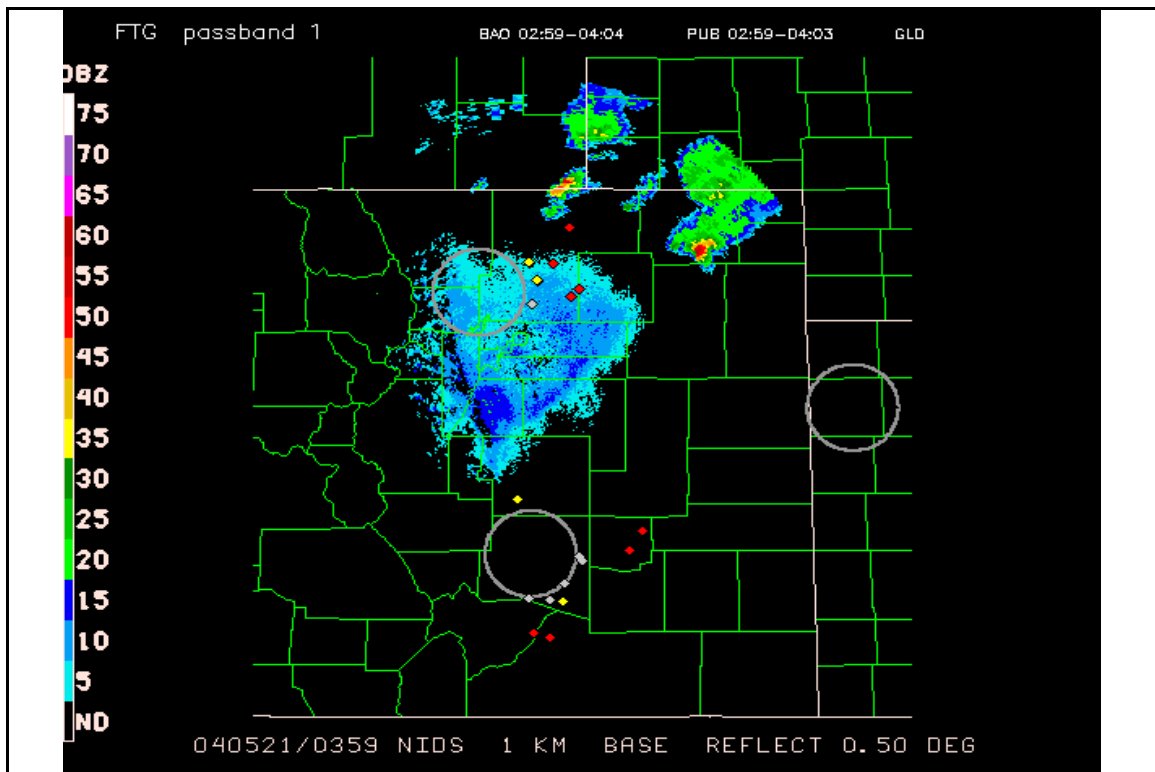


Fig. 14c. Histogram display for the ~1 h period ending at 0400 UTC.

Those results, and the results from this case, suggest that the infrasound at a passband of 1 to 5 Hz may not be producing a signal for storms that possess only a mesocyclone but no tornado. Since we cannot definitively state that there was no tornado with this case, we must hedge on this conclusion, but we hope to use this hypothesis in the examination of another supercell that did produce a confirmed tornado (results to be shown at the conference).

4. 9 JUNE 2004 CASE

This was an active severe weather day with five tornado reports (Fig. 15), four of which were weak and mostly short-lived, followed later in the day by a strong tornado that produced damage in the town of Sterling, located in the northeast corner of Colorado. The overall evolution of storms on this day was considerably more complex than on 20-21 May, and as a result we are still analyzing the details of the radar data, which we plan to present at the conference. In this section, then, we will briefly discuss the ISNet data along with some low-level radar scans, and speculate on some differences between what is shown versus the previous case.

The sounding from Denver from 1200 UTC on 9 June was not quite as impressive as the one from 20 May, but there was still enough vertical wind shear in the environment, as well as potential instability, to support possible supercell storms (Fig. 16). Although a boundary (the Denver

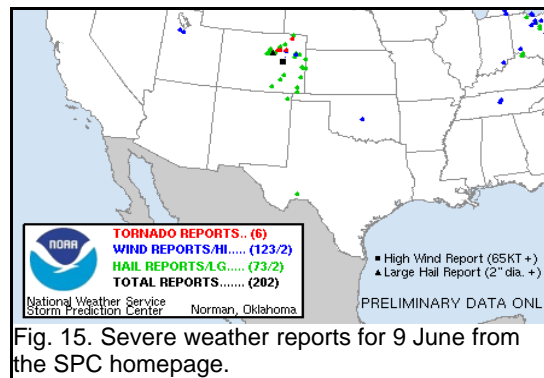


Fig. 15. Severe weather reports for 9 June from the SPC homepage.

convergence zone associated with a Denver Cyclone) was important to the development of the initial storm on 20 May, the incipient supercell quickly moved away from the boundary in the strong steering flow. A difference then on 9 June was the presence of interacting boundaries that appear to have had an important influence on the development of at least the first three tornadoes on this day. The details of the radar evolution are shown in the low-level radar reflectivity scans in Fig. 17. Except for Fig. 17a, the times of the radar scans shown correspond to the times of the first four tornadoes. The first storm of interest developed very close to the radar after 2100 UTC near an eastward-advancing north-south boundary. This boundary, and another more east-west pre-existing boundary, are distinctly shown in the clear-air reflectivity echo in the images in Fig. 17. The first tornado was reported with the storm located just east of the radar at 2215 UTC, near the time of

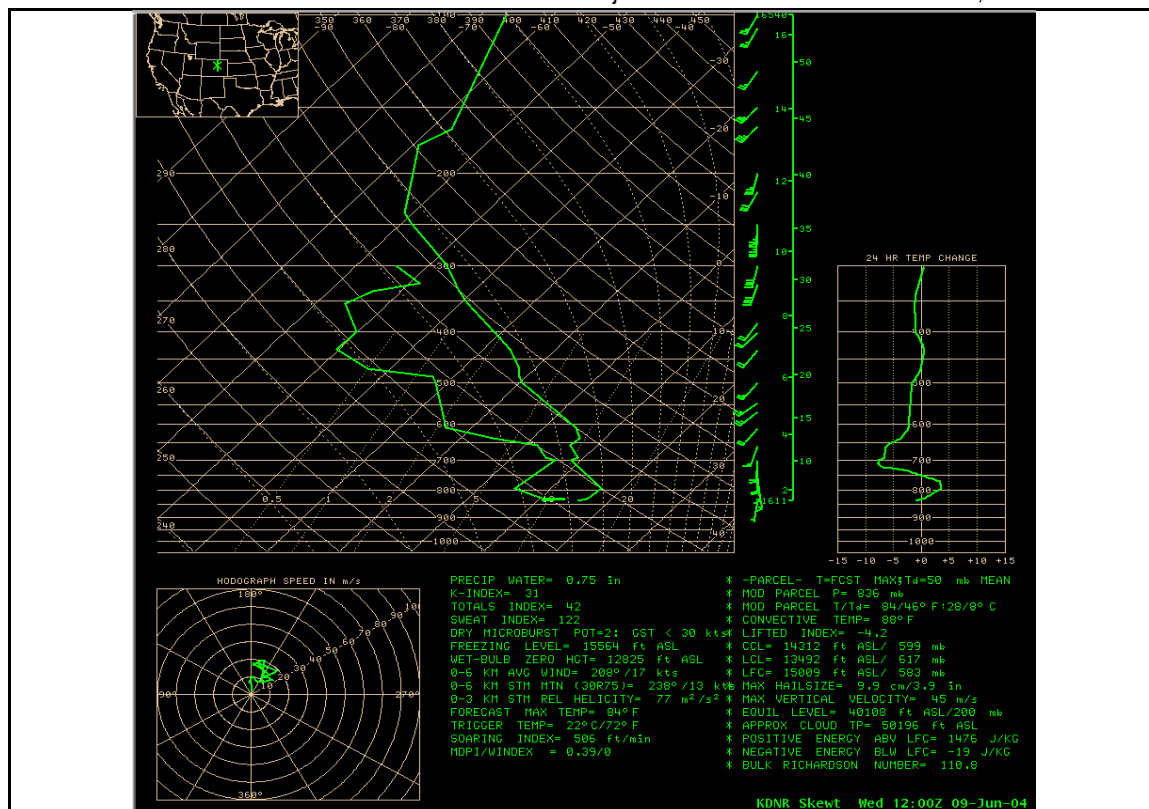


Fig. 16. Denver sounding for 1200 UTC on 9 June 2004.

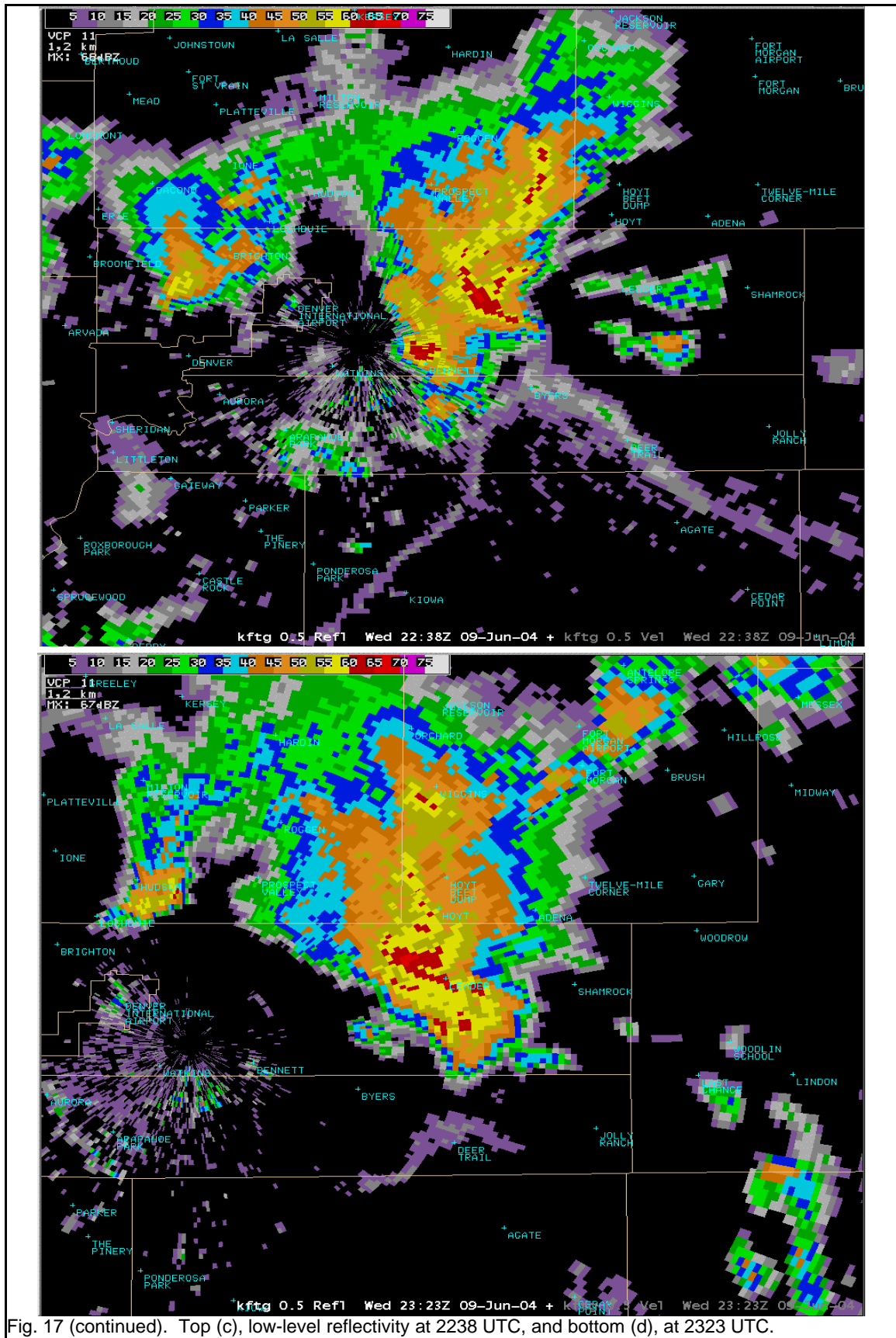


Fig. 17 (continued). Top (c), low-level reflectivity at 2238 UTC, and bottom (d), at 2323 UTC.

Fig. 17b, and apparently right at the intersection of the two boundaries. This was most likely a non-supercell tornado (Brady and Szoke 1989; Wakimoto and Wilson 1989), judging by the presence of the boundaries and spotter reports. Twenty minutes later two other tornadoes occur with this same storm, one fairly weak, one apparently along the east-west boundary and the other possibly closer to the intersecting boundaries (Fig. 17c). A somewhat stronger tornado occurs at 2321 UTC (Fig. 17d) as the storm begins to progress eastward, but still as it was interacting with the pre-existing east-west boundary. All of these tornadoes may have been non-supercell types (this will be confirmed through more detail radar analysis). Later that evening, however, a more organized storm embedded within an overall line of echoes produced a significant (F1) tornado that caused damage in the town of Sterling, in far northeastern Colorado (near the time of the radar image in Fig. 18). The tornadic storm in Fig. 18 is the hook-shaped echo with the 55-60 dBZ (yellow) core.

For this case the infrasound signals were much stronger and more consistent than those from the 20 May case. Even the “standard” display in use at the test site WFOs revealed a strong signal, as shown in Figs. 19 and 20. The correlation coefficient time series display that was shown in Fig. 13 for the 20 May case is repeated here for the period of 2200-2300 UTC on 9 June (Fig. 21), along with a time series of the azimuth of the received signal (as in Fig. 10). A short but strong

signal is seen near the time of the first tornado at 2215 UTC, followed by a more consistent strong signal that persists up to the time of the next two tornadoes around 2235 UTC. Although the strength of the signal goes down, a consistent signal continues to come from the echo after 2230 UTC. This signal continues into the following hour (Fig. 22), and then increases in strength before the tornado observed at 2321 UTC.

Clearly there is a much stronger and consistent signal for this event when four apparently fairly small tornadoes were observed. The signal seen was quite different than that from the very strong supercell storm from 20 May. The eventual supercell that developed later on during the evening of 9 June did not appear to be as intense as the one on 20 May (although this is still to be determined), but it produced a significant tornado that went through the town of Sterling, Colorado at 0125 UTC. The final set of ISNet time series, similar to Fig. 21, is repeated for the 0100 to 0200 UTC time period in Fig. 23. A very consistent signal is shown from the azimuth pointing toward the Sterling storm (Fig. 23b), while the correlation coefficient (Fig. 23a) increases before the observed time of the tornado. The strong signal still shown after the apparent time of the tornado is in part caused by the time taken for sound to travel from this storm, which by 0130 UTC is about 200 km from the radar.

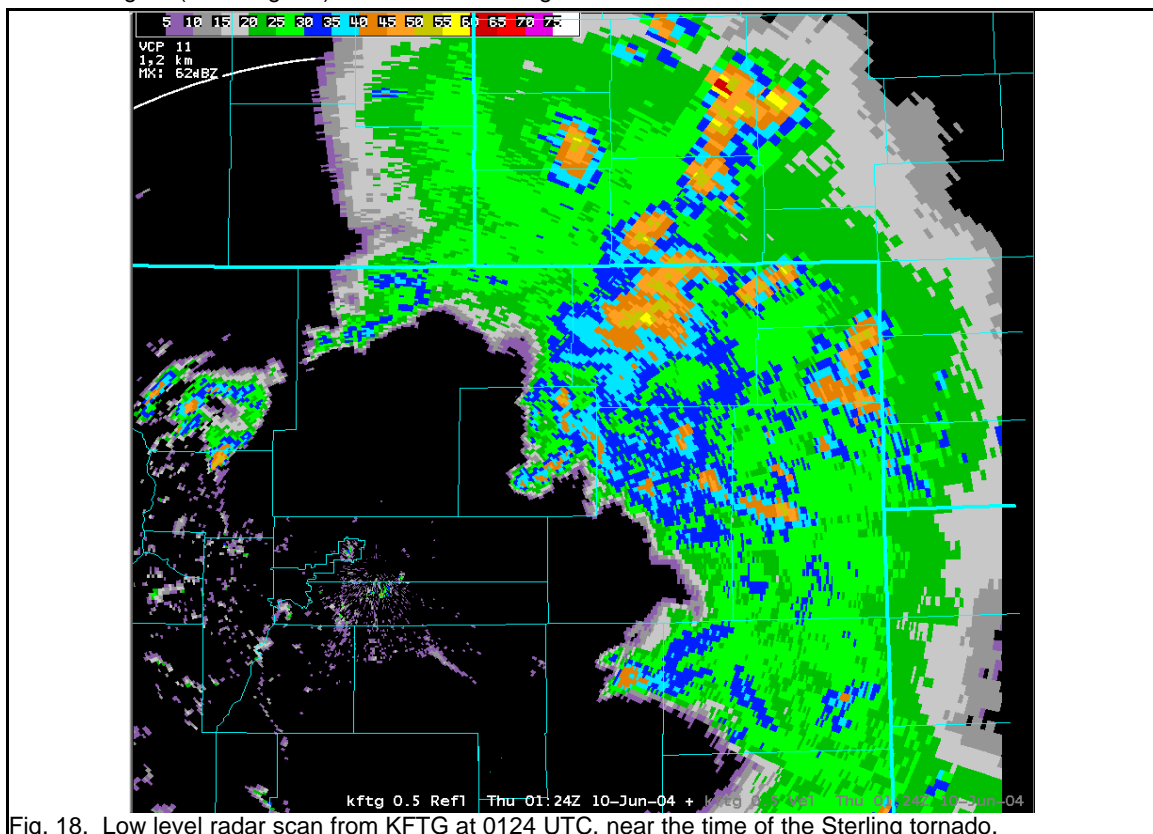


Fig. 18. Low level radar scan from KFTG at 0124 UTC, near the time of the Sterling tornado.

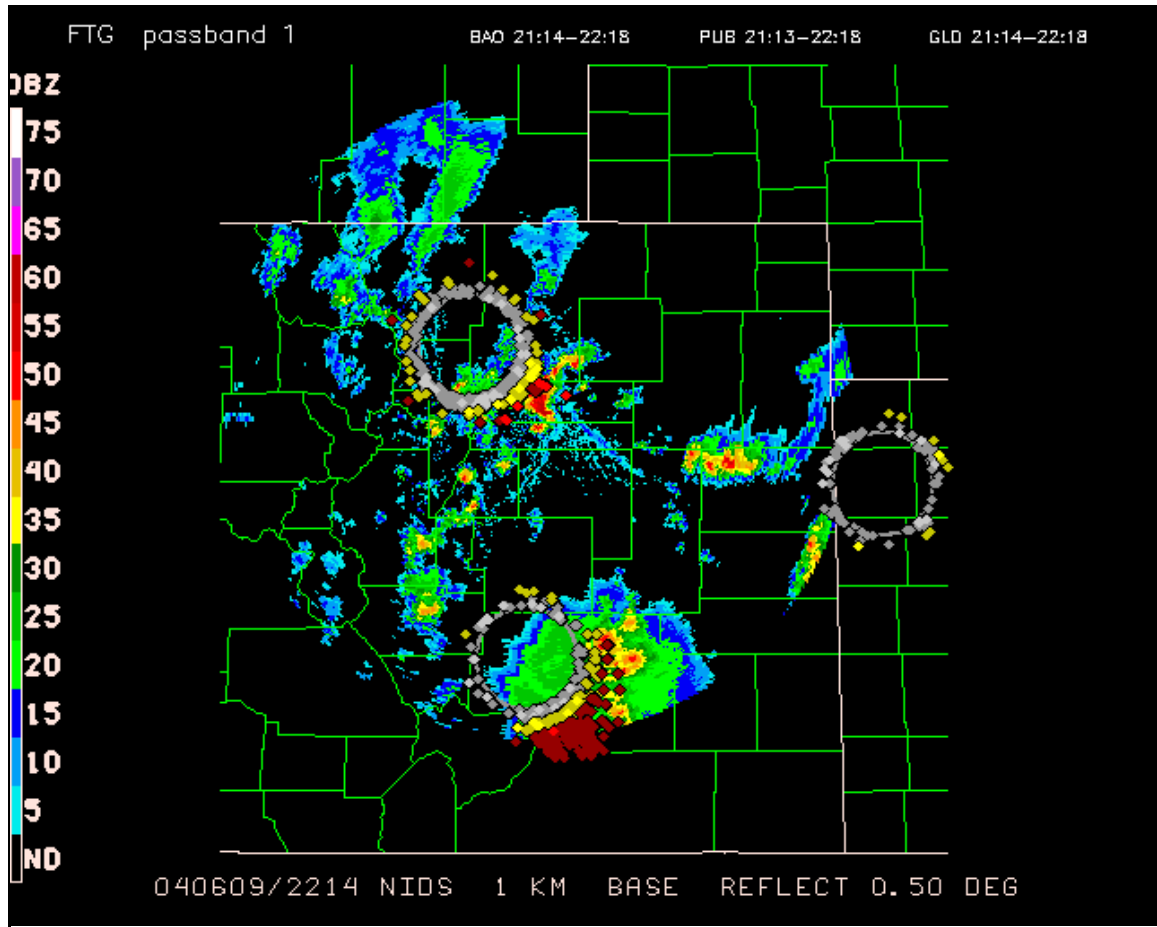


Fig. 19. "Standard" ISNet display (as in Fig. 8), for the ~1 h period ending at 2214 UTC on 9 June.

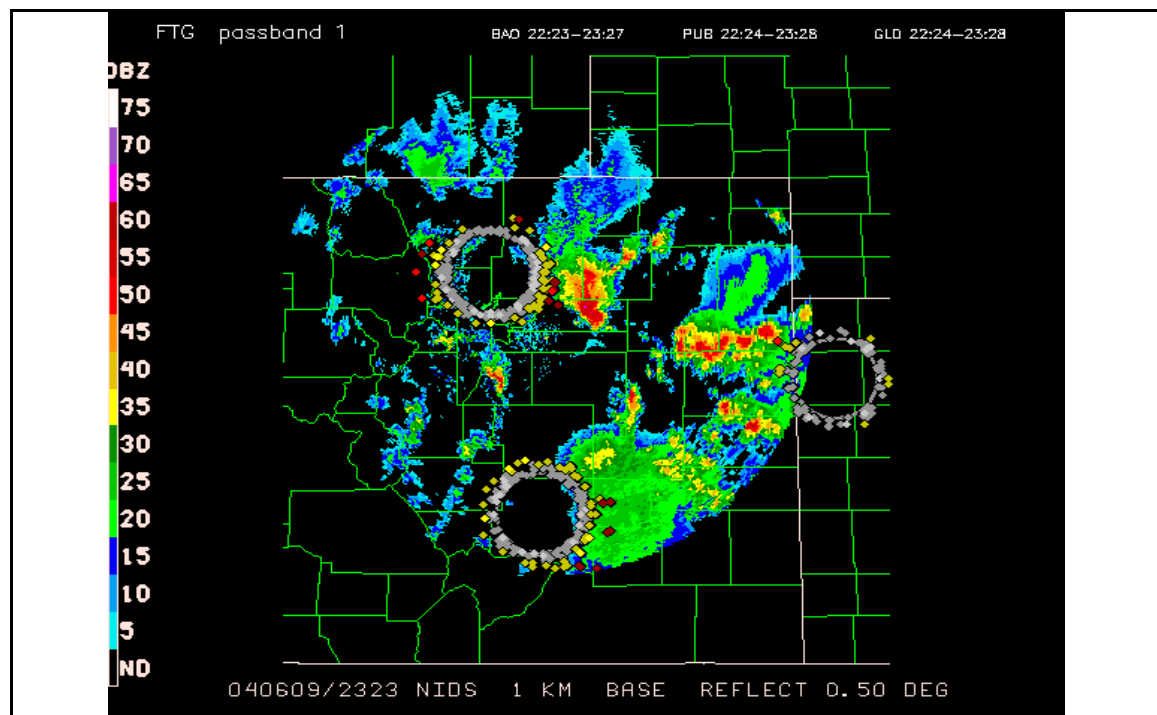


Fig. 20. As in Fig. 19, but for the ~1 h period ending at 2323 UTC.

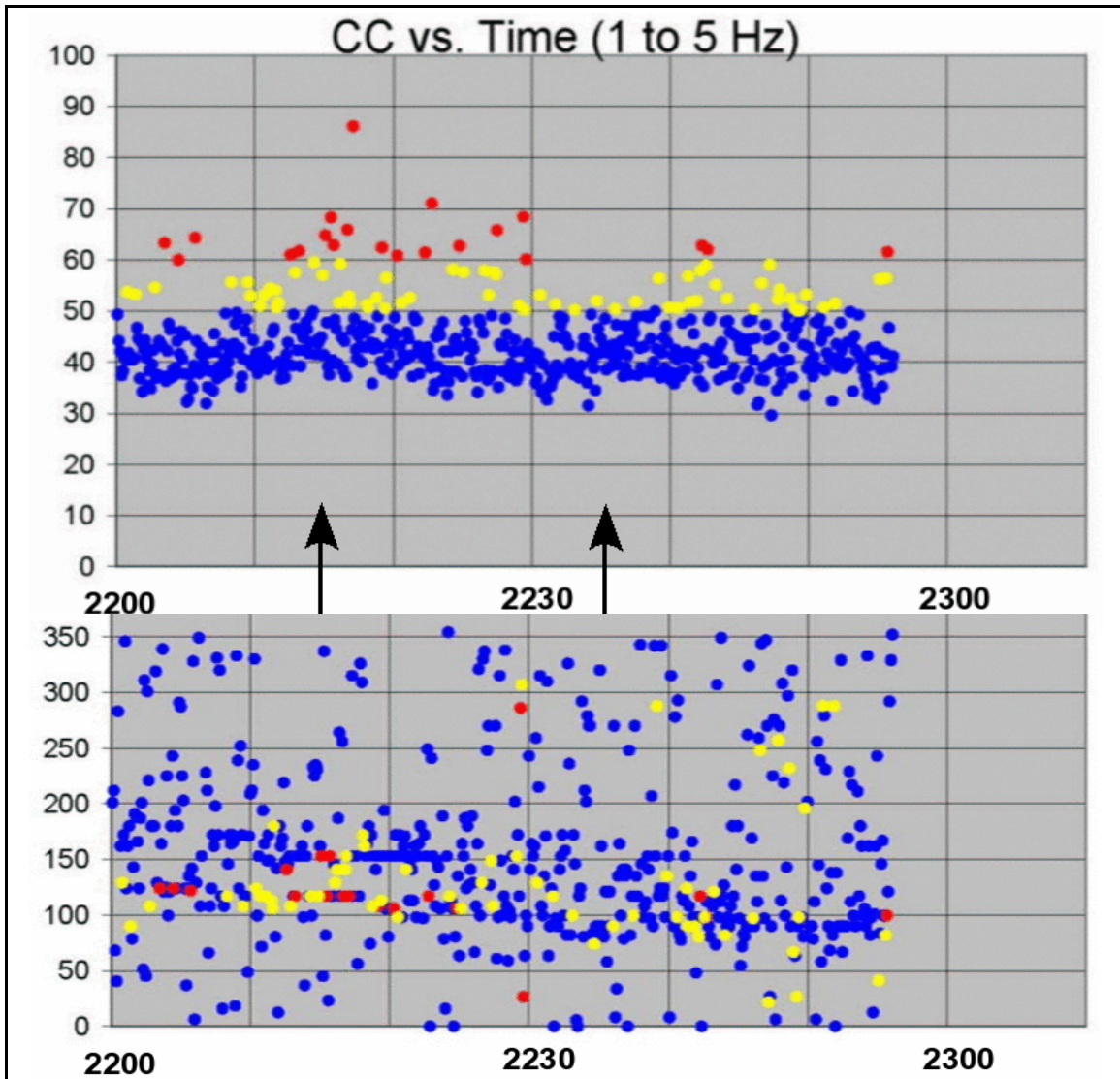


Fig. 21. Time series displays of correlation coefficient (a, top), as in Fig. 13, and signal azimuth (b, bottom), as in Fig. 10, for the ~1 h period ending near 2300 UTC. Arrows indicate times for reported tornadoes.

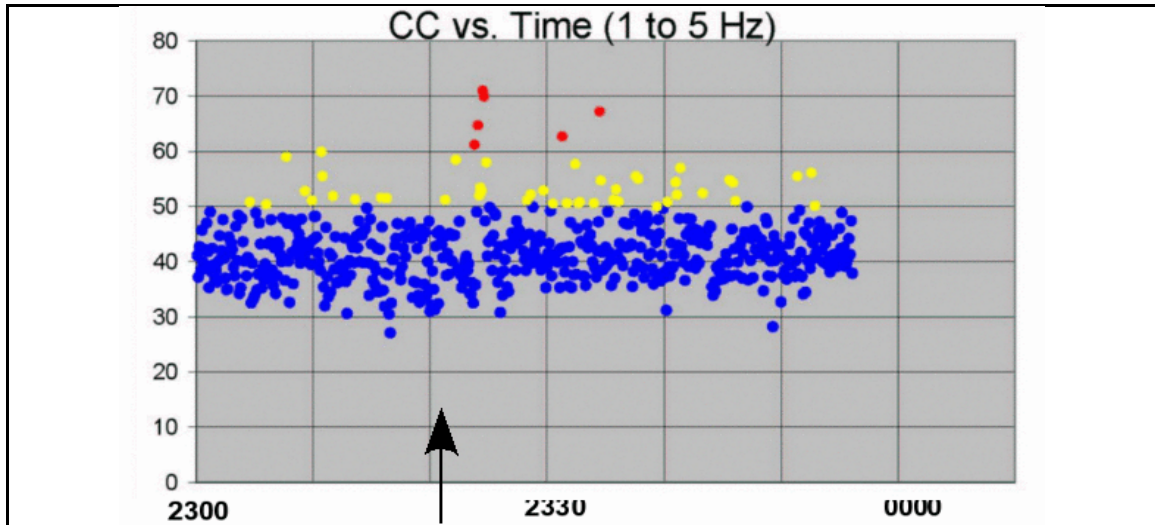


Fig. 22. Time series displays of correlation coefficient for the ~1 h period ending at 0000 UTC on 10 June.

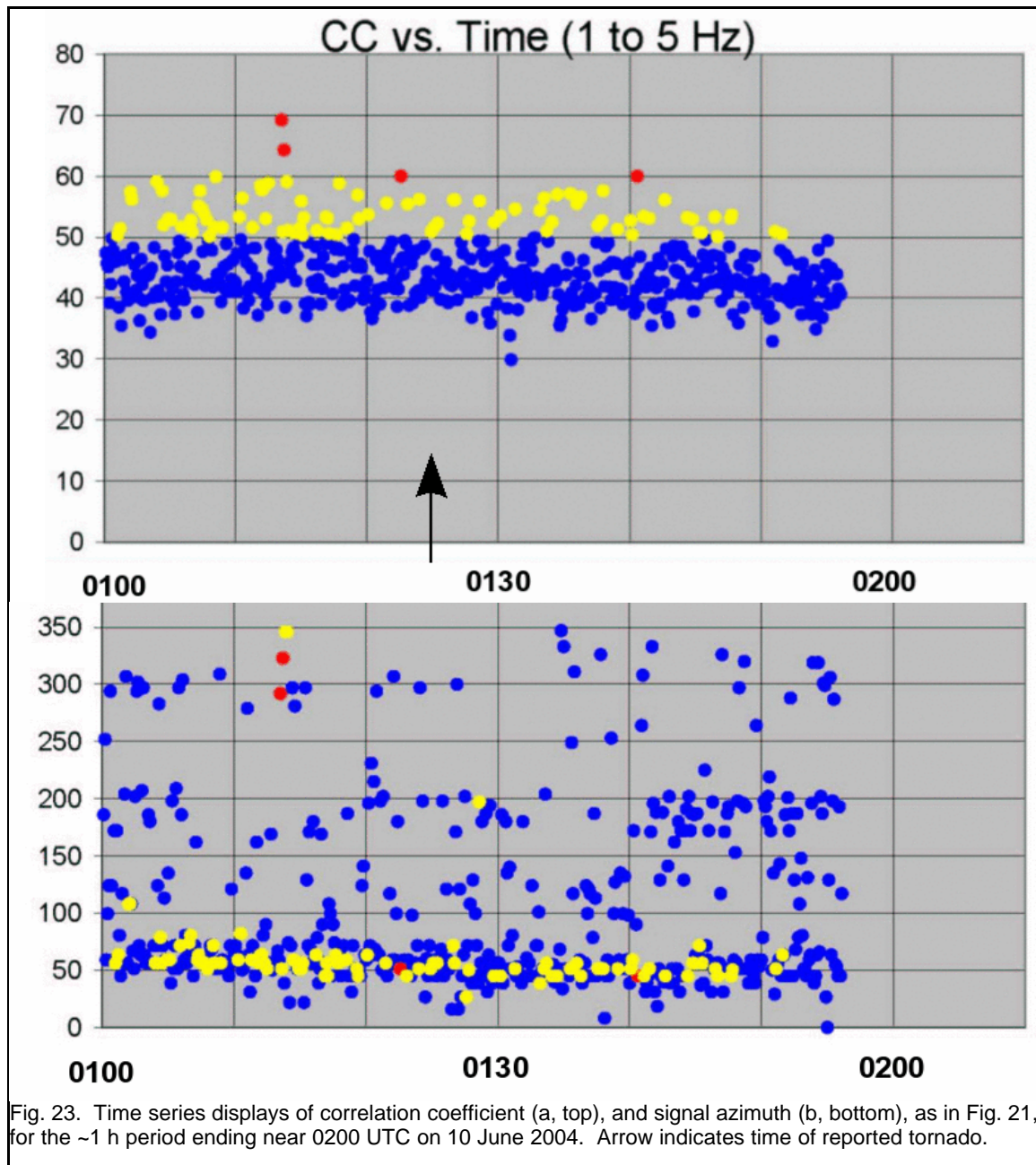


Fig. 23. Time series displays of correlation coefficient (a, top), and signal azimuth (b, bottom), as in Fig. 21, for the ~1 h period ending near 0200 UTC on 10 June 2004. Arrow indicates time of reported tornado.

5. CONCLUDING REMARKS

The potential value of infrasound detection as an aid in predicting tornadogenesis is currently being tested with experimental displays at three NWS WFO sites, Boulder, Pueblo, and Goodland. A number of intriguing correlations have been suggested by comparing ISNet output with occurrences of tornadoes, as documented by Bedard et al (2004). There remain, however, many questions as to exactly what the ISNet signals mean in terms of storm structure, tornado evolution, and tornadogenesis, as well as how the signals compare to what is observed with Doppler radar, the standard tool for NWS tornado warnings.

In this paper we have attempted to correlate the ISNet signals with detailed radar output, initially for an isolated supercell storm that may have produced tornadoes. A similar study is underway for another case of confirmed apparent non-supercell tornadoes, followed by a significant damaging supercell tornado.

Results at this time are intriguing; there was not much of an ISNet signal for the strong supercell storm on 20 May, but then it is quite possible this storm did not produce an actual tornado. On the other hand, strong signals were recorded on 9 June, and appear to precede by up to 30 min or more the occurrence of five tornadoes this day.

The strong signals occur from both the small tornadoes (non-supercellular tornadoes, aka "landspouts"), as well as from the supercell-produced tornado. Further results for the 9 June case, and possibly another very interesting tornadic day that occurred somewhat out of season on 9 August 2004 and was well documented by storm chasers, will be shown at the conference.

Thus far forecasters at the Boulder WFO have not found the ISNet data to be useful for very many of the severe events during the 2004 season. There are a number of reasons for this. Certainly the unfamiliarity with this type of data and what it means is an issue. Another big problem appears to be figuring out how to make a useful and meaningful display of the data, and there has been considerable confusion with the current basic display (as shown in Figs. 6, 8, 19 and 20). Some new types of displays, illustrated in this paper, may be used for testing next season and could help immensely. Further study, correlating infrasound data with visual and detailed radar observations for more cases, will provide a much improved understanding of what we may be observing. Taken together, the changes and additional information could encourage forecasters to further examine the ISNet data.

At this point there does appear to be potential for receiving useful information from an infrasound detecting system that may aid in the issuance of tornado warnings. Although we are in no position at this time to definitively state the value of an infrasound detecting system, based on the limited results thus far, the information from such a system may prove particularly useful for discriminating between supercells that produce tornadoes and those that do not, as well as potentially helping to discern non-supercell tornadoes. Both of these issues are gaps in the current Doppler radar capabilities.

6. ACKNOWLEDGEMENTS

We thank Susan Carsten of FSL for a technical review of this manuscript and Ed Tollerud of FSL for an internal scientific review.

7. REFERENCES

- Bedard, A.J., B.W. Bartram, A.N. Keene, R.T. Nishiyama, and D.C. Welsh, 2004: The infrasonic network (ISNet): Background, design details, and display capability as an 88D adjunct tornado detection tool. *22nd Conf. On Severe Local Storms*, Hyannis, MA, Amer. Meteor. Soc., Paper 1.1.
- Brady, R.H., and E.J. Szoke, 1989: A case study of nonmesocyclone tornado development in Northeast Colorado: Similarities to waterspout formation. *Mon. Wea. Rev.*, **117**, 843-856.

Brooks, H.E., 2004: Tornado-warning performance in the past and future, a perspective from signal detection theory. *Bull. Amer. Meteor. Soc.*, **85**, 837-843.

Szoke, E. J., M.L. Weisman, J.M. Brown, F. Caracena, and T.W. Schlatter, 1984: A subsynoptic analysis of the Denver tornadoes of 3 June 1981. *Mon. Wea. Rev.*, **112**, 790-808.

Wakimoto, R.M., and J.W. Wilson, 1989: Non-supercell tornadoes. *Mon. Wea. Rev.*, **117**, 1113-1140.